Uncertainty of Line Segments Extracted from Static SICK PLS Laser Scans

Albert Diosi and Lindsay Kleeman
Intelligent Robotics Research Centre
Department of Electrical and Computer Systems Engineering
Monash University, Clayton, VIC 3168, Australia
{Albert.Diosi,Lindsay.Kleeman}@eng.monash.edu.au

Abstract

Knowing the uncertainty of measurements is important for sensor fusion using Kalman filters. Our sensor of interest is the Sick PLS101-112 laser range finder. We present an approach for straight line parameter estimation in polar coordinates that results in a simple covariance estimate and a worst case systematic line parameter error model based on a range error model backed up by experimental data. We show that our random and systematic line error models match experimental data most of the time. We also demonstrate that systematic line parameter errors can be larger than the random ones.

1 Introduction

Mobile robots that build their own maps whilst using them for localization represent an important step towards creating useful autonomous mobile robots. We are planning to perform simultaneous localization and mapping (SLAM) by fusing corners, edges and line segments measured by a laser range finder and advanced sonar sensors. When fusing using Kalman filters, measurements are weighted by their uncertainty. The advanced sonar sensors are capable of measuring the range and bearing of planes, corners and edges with $\sigma_{bearing} \approx 0.1^\circ$ and $\sigma_{range} \approx 0.2\ mm$ [Kleeman, 2002]. The sonar precision level motivates the work in this paper to determine the errors in estimating line segments measured by a laser scanner. We use the common Sick PLS101-112 laser scanner for experiments in this paper.

Line parameter error estimates depend on the line fitting methods and on range error models. There are several approaches for fitting lines to range data in the literature. In [Horn and Schmidt, 1995] Hough transformation is used to find planes representing walls in 3D laser scans. Using least squares minimization, a plane in its general form was fitted to the points of the wall. The intersection of vertical planes with the floor was calculated and the resulting line was converted into its normal form. The uncertainty of the line parameters were calculated using Taylor series expansion. However, the measured points were assumed to be affected only by non-systematic uncorrelated noise in the bearings and in the range.

In [Nygårds, 1998], a local Cartesian coordinate system is placed into the center of gravity of a line segment, with the vertical axis pointing in the opposite direction, than that of the laser. The regression coefficient of the line is determined by linear regression, which is sensitive to noise for nearly vertical lines. From knowledge of the centre of gravity and the regression coefficient, the angle and perpendicular distance parameters of the normal form of a line are calculated. The covariance of the angle and distance estimate of the line is derived, under the assumption of error free laser bearings.

Jensfelt [Jensfelt, 2001] uses the solution given in [Deriche *et al.*, 1992], where the angle and distance parameters of a line are estimated by minimizing the sum of square perpendicular distances of the points from the line in Cartesian coordinate system. A simple covariance estimate is given of the line parameters, assuming uniform covariance of each point. However this assumption is only valid for short line segments if data is obtained from a laser range finder utilizing a rotating mirror.

Similarly to [Jensfelt, 2001] in [Arras and Siegwart, 1997] the authors minimized the sum of square perpendicular distances of points to a line in Cartesian coordinate system, however their solution accounts for nonuniform weights of points. They also show an equivalent solution with polar coordinates, which was used to derive a line parameter covariance estimate assuming only errors in the range measurements.

Contrary to the previously described methods, in [Taylor and Probert, 1996] the authors take advantage of the description of a line in polar coordinate system, and minimize the sum of square errors of reciprocal ranges. However, we believe that due to the use of the reciprocal of the range, their approach implicitly weights closer points more than further ones.

In all of these papers, systematic errors are neglected in line estimates, and little experimental evidence is presented to support error models. Systematic errors are shown in this paper to be a significant component of the final errors in line parameters.

One of the sources of systematic errors in line parameter estimates are systematic errors in the range measurements. In the literature there are papers on laser range finder characterization covering Amplitude and Frequency Modulated Continuous Wave and time-of-flight (TOF) lasers. This paper concentrates on TOF lasers such as the PLS itself. In [Reina and Gonzales, 1997] and [Ye and Borenstein, 2002]) the authors investigate the accuracy of a laser range finder from Schwartz Electro-optics Inc., and a Sick LMS 200. They found that systematic errors in range changed with the time of operation, the reflectivity of the surface, and the incidence angle of laser beam and target surface. In [Reina and Gonzales, 1997] a scale factor error is reported.

In practice, uncertainty in the exact location of the laser with respect to the robot can contribute to the error in the laser measurements as well. The problem of calibrating the lasers position with respect to the robots frame of reference is addressed in [Krotkov, 1990].

The paper is organized as follows. Firstly an approach for line parameter estimation straight in polar coordinates is presented that enables a simple line parameter covariance estimation. We also investigate how systematic range error types influence systematic line errors. Our range error models are validated with experimental data. Finally experimental validation of our systematic and random line parameter error model is presented.

2 Line Error Models

A suitable line representation is described by the following equation in a Cartesian coordinate system (X, Y):

$$x\cos\alpha + y\sin\alpha = d \tag{1}$$

where α is the angle between the X axis and the normal of the line, and $d \geq 0$ is the perpendicular distance of the line to the origin. However, x and y are a function of the angle of the laser beam (ϕ) and the measured range (r). Therefore it is often more convenient to work with a line in the laser range finder's polar coordinate system (Φ, R), where a line is represented as:

$$r = \frac{d}{\cos(\alpha - \phi)} \tag{2}$$

2.1 Random Errors

The estimation of line parameter covariance depends on the line fitting method itself. We have developed an approach for finding (α, d) with estimated uncertainty directly in the laser scanners polar coordinate system (Φ, R), at the expense of linearization.

If we linearize eq. 2 around (α_0, d_0), we get

$$r_i - r_{0i} \approx \frac{d_0\sin(\alpha_0 - \phi_i)}{\cos^2(\alpha_0 - \phi_i)}\Delta\alpha + \frac{1}{\cos(\alpha_0 - \phi_i)}\Delta d \tag{3}$$

This is restated in vector form as

$$\mathbf{\Delta r} = \mathbf{r_m} - \mathbf{r_0} = \mathbf{H_0}\mathbf{\Delta b} + \mathbf{R} \tag{4}$$

Where

$$\mathbf{H_0} = \begin{bmatrix} \cdots & \cdots \\ \frac{d_0\sin(\alpha_0-\phi_i)}{\cos^2(\alpha_0-\phi_i)} & \frac{1}{\cos(\alpha_0-\phi_i)} \\ \cdots & \cdots \end{bmatrix} \tag{5}$$

$$\mathbf{\Delta b} = \begin{bmatrix} \Delta\alpha & \Delta d \end{bmatrix}^T \tag{6}$$

$\mathbf{R}$ is a vector of measurement noise with a covariance matrix $\sigma_r^2 I$ and $\mathbf{r_m}$ is a vector containing measured ranges.

Using linear regression [Wetherill, 1986] iteratively on the linearized problem (eq. 4), we can find (α, d) which minimizes the square sum of range residuals, the following way:

$$\mathbf{r_j} = \begin{bmatrix} r_{j1} & \cdots & r_{ji} & \cdots & r_{jn} \end{bmatrix}^T = \\ = \begin{bmatrix} \cdots & \frac{d_j}{\cos(\alpha_j-\phi_i)} & \cdots \end{bmatrix}^T \tag{7}$$

$$\mathbf{H_j} = \begin{bmatrix} \cdots & \cdots \\ \frac{d_j\sin(\alpha_j-\phi_i)}{\cos^2(\alpha_j-\phi_i)} & \frac{1}{\cos(\alpha_j-\phi_i)} \\ \cdots & \cdots \end{bmatrix} \tag{8}$$

$$\mathbf{\Delta b} = \left(\mathbf{H_j^T H_j}\right)^{-1}\mathbf{H_j^T}(\mathbf{r_m} - \mathbf{r_j}) \tag{9}$$

$$\begin{bmatrix} \alpha_{j+1} \\ d_{j+1} \end{bmatrix} = \begin{bmatrix} \alpha_j \\ d_j \end{bmatrix} + \mathbf{\Delta b} \tag{10}$$

Eq. 9 yields the least squares estimate, and can be found for example in [Kay, 1993]. By initializing $\mathbf{r_j}$ with (α_0, d_0) obtained from principal component analysis (PCA), this iterative process converges quickly to values near the PCA estimate. The advantage of the above mentioned approach is that a simple covariance estimate is obtained due to the use of linear regression [Wetherill, 1986]:

$$cov(\mathbf{\Delta b}) = cov(\alpha, d) = \sigma_r^2(\mathbf{H^T H})^{-1} \tag{11}$$

where the noise in the range measurements is assumed to be zero mean white noise with a variance of σ_r^2. However the noise is not always so well behaved as will be seen in results below. The use of eq. 11 also assumes that there is no error in the measurement of ϕ_i.

2.2 Systematic Errors

When modeling the systematic error of line parameters, we consider the effects of the following systematic range error types: constant bias, bias increasing linearly with distance, bias changing with the incidence angle of target surface and laser beam and bias due to range quantization. In addition we also consider the effect of error contribution from laser plane misalignment. In our approximation, the contributions from all error sources are calculated separately while assuming knowledge of the true line parameters, and assuming no influence from other error sources. The absolute values of line parameter errors are summed up to obtain a worst-case approximation.

Error Estimation Approach

In most cases the following approach is used in the derivation of our models:

First we estimate the line parameters (α, d) from the measured bearings and ranges (ϕ_i, r_i), and assume that they are the true parameters. In order to simplify closed form derivations we normalize the line by shifting the measured bearings by $\phi_i = \phi_i - \alpha + \frac{\pi}{2}$ so the line becomes horizontal ($\alpha = \pi/2$). Normalization has no effect on the error estimates $(\Delta\alpha, \Delta d)$, because this corresponds to a shift only in a polar coordinate system.

In the next step either Cartesian or polar coordinate systems can be used.

Upon choosing the Cartesian coordinate system, we need to calculate what would be measured given the true signal and the modeled systematic error:

$$r_i = \frac{d}{\cos(\frac{\pi}{2} + \phi_i)} + \Delta r_i = \frac{d}{\sin\phi_i} + \Delta r_i \tag{12}$$

After transforming (ϕ_i, r_i) into (x_i, y_i) we use standard linear regression to find the parameters of a line in point intercept form $y = kx + q$:

$$k = \frac{n\sum x_i y_i - (\sum x_i)(\sum y_i)}{n\sum x_i^2 - (\sum x_i)^2} \tag{13}$$

$$q = \frac{\sum y_i - k\sum x_i}{n} \tag{14}$$

Because the true line is horizontal, the error in angle is $\Delta\alpha \approx k$ and the error in distance is $\Delta d \approx q - d$.

However if a polar coordinate system is adopted, we calculate $(\Delta\alpha, \Delta d)$ using one iteration of the line fitting in polar coordinate system approach modified for horizontal lines and for non-matrix calculations:

$$\Delta\alpha = \frac{\sum \Delta r_i a_i \sum a_i b_i - \sum \Delta r_i b_i \sum a_i^2}{(\sum b_i a_i)^2 - \sum b_i^2 \sum a_i^2} \tag{15}$$

$$\Delta d = \frac{\sum \Delta r_i b_i \sum a_i b_i - \sum \Delta r_i a_i \sum b_i^2}{(\sum b_i a_i)^2 - \sum b_i^2 \sum a_i^2} \tag{16}$$

where $a_i = \frac{1}{\sin\phi_i}$ and $b_i = \frac{d\cos\phi_i}{\sin^2\phi_i}$.

Finally, derivation of approximate closed form solutions can be facilitated in both coordinate systems by replacing sums with integrals just as:

$$\sum_{i=1}^{n} \sin\phi_i \approx \frac{n}{\Delta\phi}\int_{\phi_1}^{\phi_n} \sin\phi \, d\phi \tag{17}$$

where $\Delta\phi = \phi_n - \phi_1$. This step can be done if the bearing increments are sufficiently small.

Constant Identical Bias

If we assume that each range reading has a constant bias $\Delta r = r_b$ then using the error estimation in Cartesian coordinates and linearization, the following approximation of the systematic error is derived in [Diosi and Kleeman, 2003]:

$$\Delta\alpha \approx -\frac{r_b}{d}\frac{\Delta\phi G + \ln\left|\frac{\sin\phi_n}{\sin\phi_1}\right|(\cos\phi_n - \cos\phi_1)}{\Delta\phi^2 + \Delta\phi(\cot\phi_n - \cot\phi_1) + \ln^2\left|\frac{\sin\phi_n}{\sin\phi_1}\right|} \tag{18}$$

$$\Delta d \approx \frac{r_b}{\Delta\phi}\left(\cos\phi_1 - \cos\phi_n - \Delta\alpha G - \frac{d\Delta\alpha}{r_b}\ln\left|\frac{\sin\phi_n}{\sin\phi_1}\right|\right) \tag{19}$$

where $G = \sin\phi_n - \sin\phi_1$.

Bias Increasing with Range

Assuming a systematic range error proportional to distance and this error is zero for the closest measured point (r_{min}) of the line segment, then the error in range is:

$$\Delta r_i = (r_i - r_{min})k \tag{20}$$

By following the error estimation in polar coordinate system approach, we can derive the following result (see [Diosi and Kleeman, 2003]):

$$\Delta\alpha = \frac{k}{\sin\phi_{min}}\frac{BD - A\ln\left|\frac{\tan\frac{\phi_n}{2}}{\tan\frac{\phi_1}{2}}\right|}{A^2 - CD} \tag{21}$$

$$\Delta d = dk\frac{A\left(A - \frac{B}{\sin\phi_{min}}\right) - \left[D - \frac{1}{\sin\phi_{min}}\ln\left|\frac{\tan\frac{\phi_n}{2}}{\tan\frac{\phi_1}{2}}\right|\right]C}{A^2 - CD} \tag{22}$$

where ϕ_{min} is the bearing corresponding to r_{min} and

$$A = \frac{1}{2\sin^2\phi_1} - \frac{1}{2\sin^2\phi_n}, \quad B = \frac{1}{\sin\phi_1} - \frac{1}{\sin\phi_n}$$

$$C = \frac{1}{3}\left(\cot^3\phi_1 - \cot^3\phi_n\right), \quad D = \cot\phi_1 - \cot\phi_n$$

Bias Changing with Incidence Angle

Assuming systematic range measurement errors which depend on the angle β between the laser beam and the target surface normal as follows:

$$\Delta r_i = w|\tan\beta_i| \tag{23}$$

then for a normalized line we can describe the range error as:

$$\Delta r_i = w|\cot\phi_i| = ws_i\cot\phi_i \tag{24}$$

Where $s_i = sign(\cot\phi_i)$.

Using the error estimation approach in polar coordinates derives the following result (see [Diosi and Kleeman, 2003]):

$$\Delta\alpha = \frac{ws}{d}\frac{EA - FD}{A^2 - \frac{1}{3}(\cot^3\phi_1 - \cot^3\phi_n)D} \tag{25}$$

$$\Delta d = ws\frac{FA - EC}{A^2 - \frac{1}{3}(\cot^3\phi_1 - \cot^3\phi_n)D} \tag{26}$$

where

$$E = -(t+1) + \frac{1}{\sin\phi_1} + \frac{t}{\sin\phi_n} \quad (27)$$

$$F = \frac{\cos\phi_1}{2\sin^2\phi_1} + t\frac{\cos\phi_n}{2\sin^2\phi_n} + \frac{1}{2}\ln\left|\frac{\tan\frac{\phi_1}{2}}{\left(\tan\frac{\phi_n}{2}\right)^{-t}}\right| \quad (28)$$

and $s = 1,\ t = 1$ for $\phi_1 \leq \pi/2 \leq \phi_n$; $s = 1,\ t = -1$ for $\phi_1, \phi_n \leq \pi/2$ and $s = -1,\ t = -1$ for $\phi_1, \phi_n \geq \pi/2$.

Quantization Bias

Assume that the mean quantization error in range measurements can be described by:

$$\Delta r_i = b\sin\left((r_i' - Q(r_i'))\frac{2\pi}{q_r}\right) \quad (29)$$

where b is a constant depending on the range quantization step q_r and the random noise entering the quantizer, r_i' is the true range and $Q(r_i')$ represents the quantized r_i'. Unfortunately we can not calculate the errors in the line parameters directly, because r_i' is unknown. However, if we assume that our estimated range r_i differs from r_i' only by a constant, which causes a phase shift ϵ in eq. 29, then we are able to estimate the maximum possible line parameter error, by varying ϵ. We can rewrite eq. 29 as:

$$\Delta r_i = b\sin(\delta_i + \epsilon) \quad (30)$$

where $\delta_i = (r_i - Q(r_i))\frac{2\pi}{q_r}$. By substituting eq. 30 into eq. 15 and solving $\frac{\partial\Delta\alpha}{\partial\epsilon} = 0$, we can find ϵ at which the angle error reaches an extreme:

$$\epsilon_m = atan\frac{\sum a_i b_i \sum a_i\cos\delta_i - \sum a_i^2 \sum b_i\cos\delta_i}{\sum a_i b_i \sum a_i\sin\delta_i - \sum a_i^2 \sum b_i\sin\delta_i} \quad (31)$$

Note, that when evaluating eq. 31, the laser bearings have to be normalized per se. To find out the extreme of the angle error, we need to substitute ϵ_m back into eq. 30, and then substitute Δr_i into eq. 15. Using an analogous procedure, an extreme of Δd can be also found.

A closed form solution is difficult since $Q(r)$ is a step-like function that makes integration intractable.

Laser Plane Misalignment

We found that in certain circumstances caused by for example non-equal tire pressures of the robot or faulty caster wheel design, the laser plane may not always be parallel with the floor. By the use of homogeneous transformation and assuming walls perpendicular with the floor, we have derived a formula (see [Diosi and Kleeman, 2003]) describing the line parameter error due to the mentioned error source, and found the errors induced by this source can be neglected.

Figure 1: SICK PLS101-112 laser range finder.

3 Laser Error Models

3.1 Description of the Sick PLS Laser Scanner

The laser scanner mounted on our robot is a Sick PLS 101-112 (see fig. 1). Even if the PLS series is not the latest, it probably still belongs to the most commonly used laser scanners in mobile robotics.

A rotating mirror inside the PLS sensor deflects an infrared laser beam in the range from $0°$ to $180°$ [GmbH,]. Distance is determined by measuring the time of flight of the emitted laser pulses. The resolution of the sensor is 5 cm in the distance, and maximally $0.5°$ in the angles. The worst case error according to [GmbH,] is 94 mm at the distance of 2 m and 131 mm at 4 m. One $180°$ scan takes 40 ms to complete. The maximum range of the sensor is 50 m. Measurements from the sensor are transmitted to a PC through a serial line.

The patent [Wetteborn, 1993] of the Deutches Patent Amt describes the operation of a laser range finder, which is very similar to the PLS. Therefore we assume, that the PLS and the patent [Wetteborn, 1993] are related. The laser range finder described in [Wetteborn, 1993] works the following way: A laser source sends out a pulse of 3.5 ns duration and a counter of 330 ps resolution is started. The 330 ps time resolution results in 5 cm distance resolution. The returned pulse is detected by a photo receiver. The output from the receiver is fed into a comparator. When the received signal is 7 times larger than the average noise level of the photo receiver, the output of the comparator stops the counter. Comparing the output of the photo receiver with multiples of the average noise level helps keep false detection rate low.

Returning light pulses with different light intensities generate signals on the photo detector with different rise times. In an example from [Wetteborn, 1993], the change in the rise time generates a 20 cm error in the range measurement. To correct for this error, a peak detector consisting of ECL comparators is employed to discriminate between 6 levels. The output of the peak detector is fed into a microprocessor, where the time of flight is compensated for the rise time error. However as shown below, the 6 level resolution results in easily detectable errors.

3.2 Range Errors

We propose that the range errors of the PLS can be related to four main sources: errors due to varying returned signal strengths, errors due to change in the electrical properties of the lasers components with temperature, random electrical noise in the receiver electronics and the measurement of time of flight with finite resolution which has the same effect as a truncating quantizer. Therefore the range error of the PLS is described locally, i.e. for short line segments with uniform surface properties and with the shortest range of r_{min} as:

$$\Delta r \approx r_b + k(r' - r_{min}) + w\,|\tan\beta| + \\ + b\sin((r' - Q(r'))\frac{2\pi}{q_r}) + r_n \qquad (32)$$

where r_b is bias which is constant for all readings with uniform surface properties. The linear term accounts for signal strength reducing with distance. If a laser beam illuminates a Lambertian surface, the received light intensity is assumed to decrease with range. We assume that the change in the rise time due to signal strength is linear at least for small changes. The next term approximates the effect of the incidence angle β of the laser beam and the target surface normal on the signal strength and thus the rise time. The character of the function was determined experimentally.

The last two terms in eq. 32 account for quantization and random errors in the electronics. In our model the true range r' together with white noise $r_{nr} \sim N(0, \sigma_n^2)$ enters an ideal truncating quantizer. Using the same approach as described in [Brown, 1991], the following equations can be derived that describe the mean and variance of error in the truncating quantizer output if r' is given:

$$P(r_i|r') = F\left((i+1)\,q_r - r'; 0; \sigma_n^2\right) - F\left(iq_r - r'; 0; \sigma_n^2\right) \qquad (33)$$

$$E(r_q - r') = \sum_{i=-\infty}^{+\infty} \left(iq_r - r'\right) P(r_i|r') \qquad (34)$$

$$Var(r_q - r') = \sum_{i=-\infty}^{+\infty} \left(iq_r - r'\right)^2 P(r_i|r') - \left[E(r_q - r')\right]^2 \qquad (35)$$

where $P(r_i|r')$ is the probability of the sensor returning range r_i given the true range r', F is the cumulative distribution function of a normal random variable, q_r is the quantization step and r_q is the output of the quantizer. When investigating the quantization effect in the output of the PLS sensor, Jensfelt [Jensfelt, 2001] presents similar equations to eq. 33,35, however he assumes a rounding quantizer, and ignores the bias in the quantization error. Figure 2 contains the results from equations 33-35, for $\sigma_n = 1.7\ cm,\ q_r = 5\ cm$. By observing fig. 2, the mean quantization error can be described as $-q_r/2$ added to eq. 29. In our model, we have assumed, that the manufacturer took care of $-q_r/2$. From fig. 2 we can also see, that the standard deviation of the noise

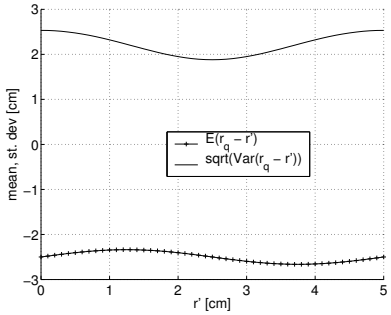

Figure 2: Simulated effect of quantization on the PLS output ($\sigma_n = 1.7\ cm$).

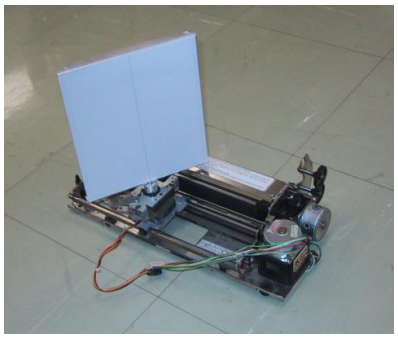

Figure 3: Laser calibration tool made from old printer.

on the output of the quantizer can be described as a sinusoid too, but for simplicity we model it as a constant σ_r. The term r_n in our model is a zero mean white Gaussian noise with variance σ_r^2.

Note that in eq. 32 the effect of internal compensation of the PLS for changing signal strength has not been modeled since we cannot access internal parameters. Therefore where we use eq. 32, the received optical magnitudes are assumed to be in one band.

4 Experimental Validation

4.1 Laser Model

Experimental Setup

The inspiration for our laser range calibrations tool came from [Ye and Borenstein, 2002], where the authors used a 4 m linear motion table with a rotating target plane mounted on it. We created a similar, but inexpensive setup (see fig. 3), by recycling the head moving mechanism of a discarded printer. We replaced the head with a 16x16 cm target plane rotated by a stepper motor from a 5.25" floppy drive. The target plane surface was covered with thick, white, non-glossy paper. The mechanism was controlled by a PC running Linux. The achieved resolution in distance and angle was 0.3 mm and $1.8°$.

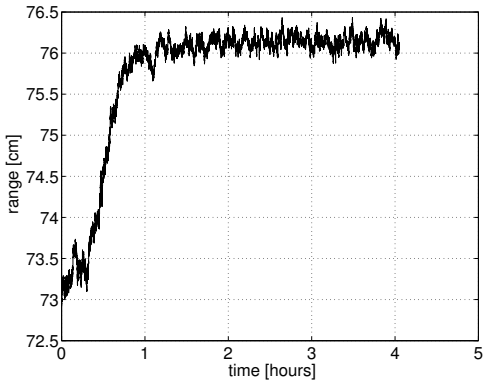

Figure 4: Change in filtered range readings during warm up.

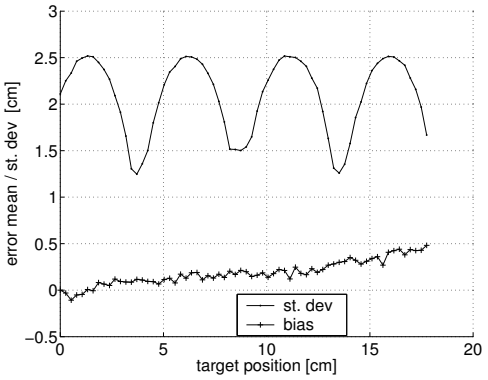

Figure 5: Measured range mean and standard deviation change on distance.

Description of the Experiments

To find out how measured ranges change with time, we collected tens of thousands of range measurements of a patch on a wall after the laser scanner was turned on. The measured ranges were filtered by a first order linear filter.

In our next experiment, using our laser range calibration tool, we measured the dependence of bias and standard deviation of the Sick PLS output on distance. The laser calibration tools longitudinal axis was aligned with a laser beam. The target plane was moved by 18 cm further away from the laser in 2.5 mm steps. After each step, the plane stayed in position for 10 minutes to enable the collection of 3000 sample points. The PLS was used in 361 point mode, and the on board averaging of measurements was turned off. Because the precise distance of the Sick PLS and the laser calibration tool was unknown, the change of bias was being measured instead of the absolute value.

Our last experiments were aimed at finding out how the range changes with incidence angle. We have aligned a laser beam on the center of the target planes axis of rotation. We have also made sure that at 0° orientation of the target plane, the laser beam was perpendicular to the plane. In the experiments we have rotated the target plane from $+70^\circ$ to -70° by 1.8° steps in each 10 min. To avoid bias from quantization to influence our measurements, we repeated the measurements after moving the target plane away from the laser by half the quantization step, eg. by 2.5 cm. In the next step we computed the average range for each angle. To allow bias due to quantization to be canceled, the average of the averages for the same angles, but different distances were calculated. Then from all the obtained results, the range value for 0° was subtracted.

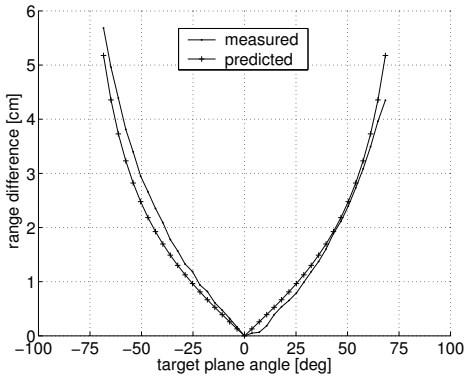

Figure 6: Measured range change depending on target plane angle - no compensation.

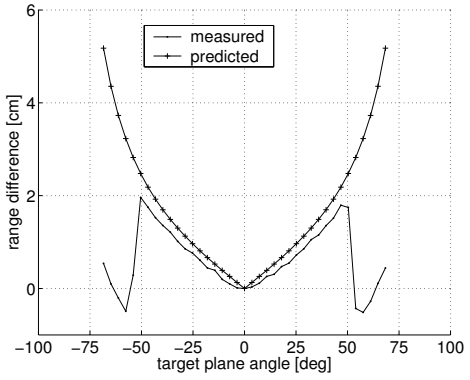

Figure 7: Measured range change depending on target plane angle - with compensation.

Results and Discussion

In our experiment aimed at measuring the change of the range with time, we have observed a 3 cm drift in the readings (see fig. 4).

The result of our experiment where we were moving the

Figure 8: Laser calibration tool – "perfect" corner.

target plane away from the laser is depicted on fig. 5. The standard deviation is a periodic function with a period of the quantization step. In half of the period the standard deviation looks like a sinusoid, which peaks at 2.5 cm. In the rest of the time it resembles a V shape.

The change in the bias, can be approximated with a linear function of distance with a slope of $0.5/18 \approx 0.03$. It is likely that just as in fig. 2 the bias has a periodic component, however it is hard to detect due to noise. It is unlikely that the rise of the bias was caused by a change in the temperature, since the PLS was allowed a 3 hour warm-up time prior the commencement of the experiment. Furthermore the range of a non moving point was also recorded during the experiment, and only about 1 mm drift was observed.

The results of our last type of experiment are depicted in fig. 6 and in fig. 7, whereas the approximated ("predicted") error was calculated as $e_r = 2|\tan\beta|$, where β is the angle of the target plane. On fig. 6 the measured error is quite close to the approximated, however on fig. 7 it seems as if at angle $\pm 50^\circ$, 2.5 cm was subtracted from the readings. A possible explanation for that is the following: as the target plane was rotated, less and less light came back to the laser scanner, causing longer and longer rise times of the output signal of the photo detector. We suspect, that at $\pm 50^\circ$ the signal level got into a different band (see section 3.1), and the laser used different compensation values. In our experiments the jump in the range readings occurred at different angles for different laser to target plane distances. Also note that the $e_r = 2|\tan\beta|$ approximation was tested only with our target plane, which was coated with a non-glossy white paper, probably giving a good Lambertian reflection. It is quite possible that surfaces with more specularity would give different error characteristics.

4.2 Line Experiments

The experiments described in this subsection are aimed at validating our line error modeling efforts.

Experimental Setup

For evaluation of the line error models a tool resembling a perfect right angle corner with 60 cm long arms (see fig. 8) was used. The angle of the corner was measured as $89.85^\circ \pm 0.3^\circ$. The surface of the corner has a rather shiny finish with visible specular reflections.

Description of the Experiments

In our experiments our robot was moving on a path resembling an arc with radius R around our "perfect" corner tool. On its course the robot stopped each Θ degrees, turned toward the corner and took about 3000 scans. Three experiments were conducted: exp. 1 with $R = 1.5\ m,\ \Theta = 5^\circ$; exp. 2 with $R = 2\ m,\ \Theta = 10^\circ$ and exp. 3 with $R = 3\ m,\ \Theta = 5^\circ$. Measurements corresponding to the corners arms were extracted from the scans and lines were fitted to them in the polar coordinate system.

For the random error test, the lines fitted to exp. 2's data was used. The covariance of line parameters was calculated for each position and arm. Then for the first line sample of each position and arm, a line covariance estimate was calculated using eq. 11, which was followed by the comparison of the covariances.

For our systematic error tests, we separately evaluated all three experiments data. However, we could only indirectly test our systematic error model for line angles the following way:
For each position, we calculated the average line parameters for both arms. Because the high number of samples, we assumed that the average angles had only systematic errors. Then the opening angle of the corner was calculated as the difference of the average angle of the two arms. For the first sample of each arm an angle error estimate was calculated by adding up the absolute values of errors calculated as described in 2.2. Errors due to laser plane misalignment were neglected. By adding up the systematic errors for both lines an error bound for the opening angle was calculated. Our error model testing consisted of checking if the measured error was within the predicted error boundaries.

Results and Discussion

A sample of each arm taken at each position is shown on fig. 9. Each line has also a number assigned to it for identification purposes. The results are shown on fig. 10, where the measured and estimated covariance matrices ($\sigma_r = 2.4\ cm$) are represented as error ellipses. The probability of a point falling inside an ellipse is about 40%.

The random error models are good enough most of the time, however in the case of lines 1,2,19, the measured covariances are considerably bigger than the predicted. The reason for this deviation is unknown. For lines 10 and 20 the error ellipses are missing, because while being processed together, line 10 did not have sufficient number of points.

The results of our systematic error experiments are shown on figures 11-13. The following error model parameters were used:

- Identical bias parameter: $r_b = 5\ cm$.
- Incidence angle error parameter: $w = 2$.

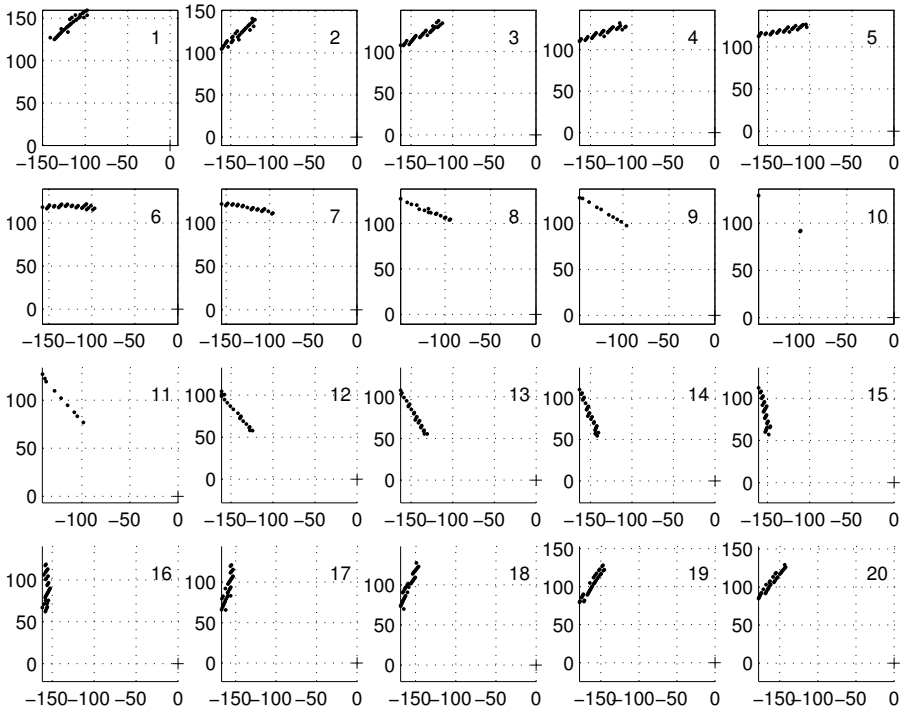

Figure 9: Sample of the raw data in Cartesian coordinate system to which lines were fitted. A "+" sign denotes the position of the laser.

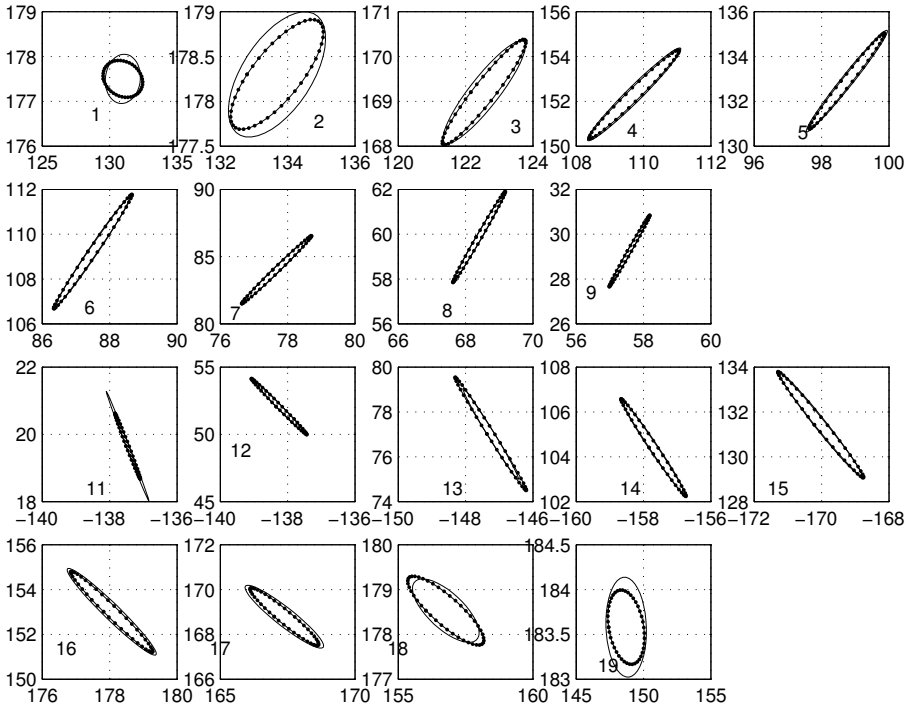

Figure 10: Error ellipses of the measured (solid line) and estimated (dotted line, $\sigma_r = 2.4\ cm$) line parameter covariances plotted in line parameter space. Horizontal axis: angles, vertical axis: distances.

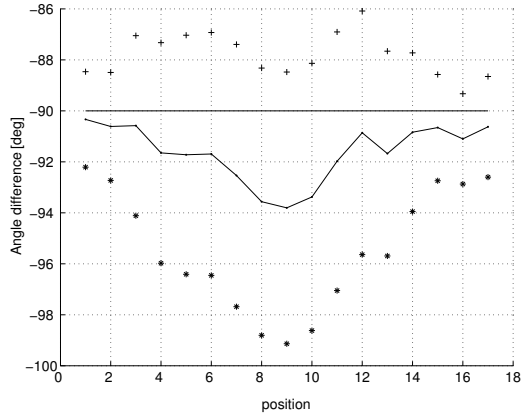

Figure 11: Systematic error model test ($R = 1.5m, \Delta\Theta = 5°$): measured opening angle of a right angle corner and error upper and lower bound estimates.

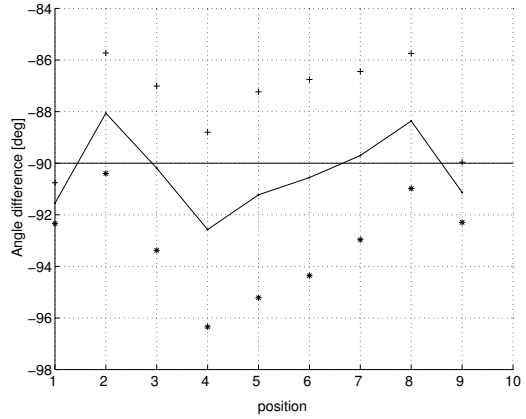

Figure 12: Systematic error model test ($R = 2m, \Delta\Theta = 10°$): measured opening angle of a right angle corner and error upper and lower bound estimates.

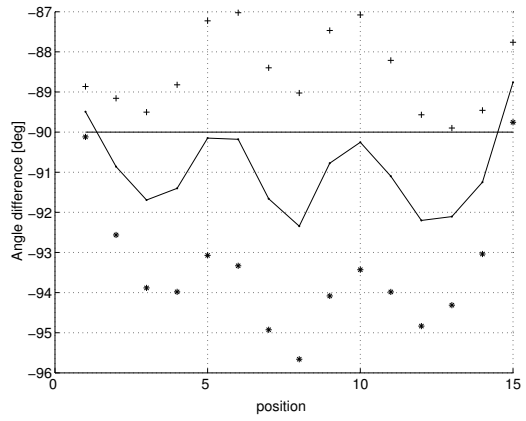

Figure 13: Systematic error model test ($R = 3m, \Delta\Theta = 5°$): measured opening angle of a right angle corner and error upper and lower bound estimates.

- Error growing with distance parameter: $k = 0.03$.
- Quantization bias parameter: $b = 0.17\ cm$.

When evaluating our random error models, we need to know that if we would have a perfect systematic error model, then either the upper, or the lower error mark would lie on the $-90°$ mark on fig. 11,12, and 13. However as we see, the errors are most of the time bigger. This is normal, because we added up the absolute values of angle errors from each error source, thus creating a worst case estimate. In reality, these errors sometimes cancel out each other. In some instances our estimated error was smaller than the measured one. It is more than likely than there are other error sources involved which were not modeled such as the error caused by wrong segmentation of the lines or the effect of the error compensation of the laser.

From fig.12 we can see that the measured systematic error reached $2°$ in several cases. Luckily we can find out if the systematic or the non-systematic error is larger for exp. 2, since exp. 2 dataset was used in the random error experiment as well. We can look up for example position 4's random error on fig. 10 by looking up line number 4's angle standard deviation which is around $1°$ and line number $10 + 4 = 14$ standard deviation, which is also around $1°$. Because the systematic error at position 4 is more than $2°$, we can conclude that systematic errors in estimated line parameters can be bigger than the random ones!

5 Conclusions

This paper contains the summary of our investigations of line segment parameter estimation from laser range data. All observations were based upon the Sick PLS 101-112 laser range finder. An approach for line parameter estimation has been developed in which parameters of a line are estimated directly in the lasers polar coordinate system, without the conversion of measurements into a Cartesian coordinate system. This line parameter estimation method allows simple and reasonably precise line parameter uncertainty estimation, which has been verified experimentally. The error models do not include effects of erroneous bearing measurements.

It has been found that errors in the estimated line parameters can have a substantial systematic error component. As we have shown the systematic error can be even larger than the random one. The sources of these errors have been identified as constant bias in the range measurements, bias changing linearly with range, bias depending on incidence angle and bias due to quantization. A worst-case systematic error model has been constructed for line parameters. Experiments using a right angle corner have shown the model to be reasonably accurate but on rare occasions under-estimates the angle error.

The applicability of our systematic error models is restricted to laser scanners with a similar principle of operation as the Sick PLS. One example is the laser scanner described

in [Reina and Gonzales, 1997]. Even if the whole systematic error model is not applicable to a particular laser scanner, parts of it could be used. For example, many lasers have a bias in their range readings which changes during warm-up.

Large systematic errors when not anticipated, can negatively influence localization and mapping performance of mobile robots. Using our random and systematic line parameter error models, we hope to improve simultaneous localization and mapping of our robot.

In the future, we plan to test the new Sick LMS laser scanner. We also plan to work on the fusion of line parameters obtained from laser and sonar measurements.

Acknowledgments

Steve Armstrong is gratefully acknowledged for technical support. The financial support of the Australian Research Council Discovery Project Grant DP0210359 is acknowledged.

References

[Arras and Siegwart, 1997] K. O. Arras and R. Siegwart. Feature extraction and scene interpretation for map-based navigation and map building. In *Proceedings of SPIE, Mobile Robotics XII*, volume 3210, 1997.

[Brown, 1991] M. K. Brown. On quantization of noisy signals. *IEEE Transactions on Signal Processing*, 39:836–841, April 1991.

[Deriche *et al.*, 1992] R. Deriche, R. Vaillant, and O. Faugeras. *From Noisy Edges Points to 3D Reconstruction of a Scene : A Robust Approach and Its Uncertainty Analysis*, volume 2, pages 71–79. World Scientific, 1992. Series in Machine Perception and Artificial Intelligence.

[Diosi and Kleeman, 2003] A. Diosi and L. Kleeman. Uncertainty of line segments extracted from static sick pls laser scans. Technical Report MECSE-26-2003, Intelligent Robotics Research Centre, Monash University, 2003. Available: http://www.ds.eng.monash.edu.au/techrep/reports/.

[GmbH,] Erwin Sick GmbH. *Opearating Instructions, PLS and PLS User Software Laser Scanner*. Waldkirch.

[Horn and Schmidt, 1995] J. Horn and G. Schmidt. Continuous localization of a mobile robot based on 3d-laser-range-data, predicted sensor images, and dead-reckogning. *Robotics and Autonomous Systems*, 14:99–118, 1995.

[Jensfelt, 2001] P. Jensfelt. *Approaches to Mobile Robot Localization in Indoor Environments*. PhD thesis, KTH, 2001.

[Kay, 1993] Steven M. Kay. *Fundamentals of Statistical Signal Processing*, volume 2. Estimation Theory. Prentice Hall, New Jersey, 1993.

[Kleeman, 2002] L. Kleeman. On-the-fly classifying sonar with accurate range and bearing estimation. In *IEEE/RSJ International Conference on Intelligent Robots and Systems*, pages 178–183. IEEE, 2002.

[Krotkov, 1990] E. Krotkov. Laser rangefinder calibration for a walking robot. Technical Report CMU-RI-TR-90-30, Robotics Institute, Carnegie Mellon University, Pittsburgh, PA, December 1990.

[Nygårds, 1998] J. Nygårds. *On Robot Feedback from Range Sensors: Reliable Control by Active Reduction of Uncertainty and Ambiguities*. PhD thesis, Lindköping University, 1998.

[Reina and Gonzales, 1997] Antonio Reina and Javier Gonzales. Characterization of a radial laser scanner for mobile robot navigation. In *IROS'97*, pages 579–585. IEEE, 1997.

[Taylor and Probert, 1996] R. M. Taylor and P. J. Probert. Range finding and feature extraction by segmentation of images for mobile robot navigation. In *Proceedings of the 1996 IEEE International Conference on Robotics and Automation*, pages 95–100, Minneapolis, Minnesota, April 1996. IEEE.

[Wetherill, 1986] G. B. Wetherill. *Regression analysis with applications*. Chapman and Hall, London, 1986.

[Wetteborn, 1993] H. Wetteborn. Laserabstandsermittlungsvorrichtung, 1993. German patent no. DE4340756A1 (November 30, 1993).

[Ye and Borenstein, 2002] C. Ye and J. Borenstein. Characterization of a 2-d laser scanner for mobile robot obstacle negotiation. In *Proceedings of the 2002 IEEE International Conference on Robotics and Automation*, pages 2512–2518, Washington DC, May 2002. IEEE.